

Adaptive Algorithm for Quantum Amplitude Estimation

Yunpeng Zhao¹, Haiyan Wang¹, Kuai Xu¹, Yue Wang¹, Ji Zhu² and Feng Wang¹

¹School of Mathematical and Natural Sciences, Arizona State University

²Department of Statistics, University of Michigan

Abstract

Quantum amplitude estimation is a key sub-routine of a number of quantum algorithms with various applications. We propose an adaptive algorithm for interval estimation of amplitudes. The quantum part of the algorithm is based only on Grover’s algorithm. The key ingredient is the introduction of an adjustment factor, which adjusts the amplitude of good states such that the amplitude after the adjustment, and the original amplitude, can be estimated without ambiguity in the subsequent step. We show with numerical studies that the proposed algorithm uses a similar number of quantum queries to achieve the same level of precision ϵ compared to state-of-the-art algorithms, but the classical part, i.e., the non-quantum part, has substantially lower computational complexity. We rigorously prove that the number of oracle queries achieves $O(1/\epsilon)$, i.e., a quadratic speedup over classical Monte Carlo sampling, and the computational complexity of the classical part achieves $O(\log(1/\epsilon))$, both up to a double-logarithmic factor.

1 Introduction

Quantum computers have the potential to perform high-speed computations based on a fundamentally different manner of storing and processing data – quantum superpositions and unitary transformations. The reader is referred to Nielsen and Chuang (2011) for a comprehensive introduction to quantum computing and Wang and Liu (2022); Wang (2022) for quantum computing in a context of statistics and data science. A major milestone in quantum computing is the discovery of a polynomial-time quantum algorithm for integer factorization (Shor, 1994), which is almost exponentially faster than the most efficient known classical algorithm (Pomerance, 1996). Another famous quantum algorithm is Grover’s algorithm (Grover, 1996), which finds with high probability the unique input to a black box function defined on $\{0, \dots, N - 1\}$ that gives a particular output, using $O(\sqrt{N})$ queries. Although only achieving a quadratic speedup over a classical brute-force search, Grover’s algorithm makes no assumption on the function other than the number of the solutions (later relaxed by Brassard et al. (2002)), and therefore has a wide range of potential applications (Ambainis, 2004; Sun et al., 2014; Zhong et al., 2021). In recent years, quantum algorithms have been developed for various domains including finance (Hong et al., 2014; Herman et al., 2022), chemistry (Cao et al., 2019), optimization (Durr and Hoyer, 1996; Kochenberger et al., 2014; Wang et al., 2016; Hu and Wang, 2020), machine learning (Ramezani et al., 2020), and high-dimensional statistics (Zhong et al., 2021), among others.

In this paper, we focus on the amplitude estimation problem introduced by Brassard et al. (2002). Suppose the basis states in a finite-dimensional complex Hilbert space¹ are partitioned into two sets, called *good* states and *bad* states. Given a quantum state, the goal of amplitude estimation is to estimate the norm of the projection of the state vector on the sub-space spanned by good states. According to the basic properties of quantum mechanics, the square of the vector norm equals the probability that a good state is obtained if the quantum state is measured. Let p denote this probability and \sqrt{p} denote the corresponding vector norm, i.e., amplitude. Amplitude estimation is different from another problem – quantum state estimation, in which the goal is to reconstruct the entire pure or mixed quantum states based upon measurements on copies of identical quantum states. The readers are referred to Artiles et al. (2005); Gill (2008); Gill and Guță (2013) for statistical methods on this problem. Amplitude estimation, by contrast, focuses on a single parameter p . Amplitude estimation has various applications, e.g., in finance (Rebentrost et al., 2018; Zoufal et al., 2019; Woerner and Egger, 2019; Egger et al., 2020), chemistry (Knill et al., 2007; Kassal et al., 2008), machine learning (Wiebe et al., 2015, 2016), and generic tasks such as Monte Carlo sampling (Montanaro, 2015) and numerical integration (Montanaro, 2015; Suzuki et al., 2020).

Brassard et al. (2002) formulated amplitude estimation as a quantum phase estimation (QPE) problem (Kitaev, 1995) and proved that QPE-based amplitude estimation can achieve a quadratic speedup over classical Monte Carlo sampling – that is, the number of oracle queries achieves $O(1/\epsilon)$ where ϵ is the desired level of precision. Suzuki et al. (2020) mentioned that QPE-based amplitude estimation involves many controlled operations, i.e., controlled Grover operators, that can be difficult to implement on noisy intermediate-scale quantum (NISQ) devices. In addition, QPE-based amplitude estimation relies on quantum Fourier transform (QFT), as mentioned by Aaronson and Rall (2020), more commonly associated with Shor’s algorithm that can achieve an exponential speedup. This raises a natural question of whether one can design an amplitude estimation algorithm, which is based only on Grover iterations and can achieve quadratic speedup. A number of Grover-based amplitude estimation algorithms have recently been proposed. Suzuki et al. (2020) built a maximum likelihood estimate for the amplitude, thereafter called maximum likelihood amplitude estimation (MLAE), based on samples generated from Grover’s algorithm with various numbers of iterations. The paper provides a lower bound of the estimation error. Wie (2019) replaced QPE by the Hadamard test in the proposed algorithm. Aaronson and Rall (2020) proposed the first Grover-based amplitude estimation algorithm with the theoretically guaranteed quadratic speedup. However, the constants in the theoretical bound are very large and the empirical estimation error is also large for practical usage (Grinko et al., 2021). Grinko et al. (2021) proposed an iterative algorithm for quantum amplitude estimation, thereafter called IQAE, and provided a proof of the correctness of the algorithm and the quadratic speedup up to a double-logarithmic factor. Grinko et al. (2021) included a sub-routine FINDNEXTK to search for search for the appropriate number of Grover iterations, which can be time-consuming. Nakaji (2020) recently proposed another Grover-based algorithm with a theoretical guarantee, but the empirical estimation error appears to be substantially larger than MLAE and IQAE (see Figure 3 of Nakaji (2020) and Figure 3 of Grinko et al. (2021)).

We propose a new Grover-based algorithm for amplitude estimation, called adaptive algorithm. The amplitude cannot be uniquely identified from the measurements if only a single circuit of

¹Hilbert space typically refers to an infinite-dimensional function space in mathematics. In quantum computing, finite-dimensional complex Hilbert spaces are usually considered, which are simply finite-dimensional complex inner product spaces.

Grover iterations is used (Suzuki et al., 2020), which creates a unique challenge – *period ambiguity* in estimation. We design an adaptive algorithm that gradually increases the number of Grover iterations such that the confidence interval² in each step can be uniquely determined based on the period estimated from the previous steps. In particular, we introduce an adjustment factor which adjusts the probability of obtaining a good state, and hence the amplitude, when the interval’s length does not exceed the period’s length but the interval overlaps with two periods. We show that the amplitude after the adjustment, and hence the original amplitude, can be estimated without ambiguity in the subsequent step. With this adjustment, our algorithm does not rely on a search sub-routine as in Grinko et al. (2021), which can be time-consuming for certain parameter values. Moreover, the number of total steps and the number of measurements in each step are easier to bound analytically. We therefore give a rigorous proof of the correctness of the algorithm and the quadratic speedup up to a double-logarithmic factor. Furthermore, we show with numerical studies that the proposed algorithm uses a similar number of quantum queries to achieve the same level of precision ϵ compared to MLAE and IQAE, but the classical part, i.e., the non-quantum part has substantially lower computational complexity. A simple analysis shows that the computational complexity of the classical part achieves $O(\log(1/\epsilon) \log(\log(1/\epsilon)))$.

We summarize the contributions as follows:

- We introduce a novel variant of interval estimation for quantum amplitudes based on Grover’s algorithm. One of the key ingredients is an adaptive adjustment factor.
- The new algorithm is easier for theoretical analysis and we prove that the number of *oracle queries* achieves $O((1/\epsilon) \log(\log(1/\epsilon)))$, which is a quadratic speedup over classical Monte Carlo sampling up to a double-logarithmic factor.
- The computational complexity of the *classical part* of the algorithm achieves $O(\log(1/\epsilon) \log(\log(1/\epsilon)))$. We show by numerical studies that the classical part has substantially lower computational costs than state-of-the-art algorithms.

The remainder of this article is organized as follows. We give a brief background review on quantum computing and on the framework for Grover-based amplitude estimation in Section 2. We explain the main idea of the algorithm in Section 3 and present the algorithm and the theoretical analysis in Section 4. The numerical comparison with state-of-the-art algorithms is given in Section 5. We conclude the paper by a discussion on future research problems in Section 6.

2 Preliminary

2.1 Brief background review on quantum computing

A quantum bit or qubit is the quantum version of the classic bit. The quantum state of a qubit is represented by a linear combination, or called superposition, of two orthonormal basis states. That

²This confidence interval is in fact for $\theta = \arcsin \sqrt{p}$. The reason of introducing this reparametrization is given in Section 2.2.

is,

$$|\xi\rangle = \begin{pmatrix} \alpha_0 \\ \alpha_1 \end{pmatrix} = \alpha_0 |0\rangle + \alpha_1 |1\rangle,$$

where $|0\rangle$ and $|1\rangle$ are the basis states:

$$|0\rangle = \begin{pmatrix} 1 \\ 0 \end{pmatrix}, \quad |1\rangle = \begin{pmatrix} 0 \\ 1 \end{pmatrix},$$

and α_0, α_1 are complex numbers, called amplitudes, satisfying $|\alpha_0|^2 + |\alpha_1|^2 = 1$. The notation $|\cdot\rangle$, called “ket”, denotes a column vector, and $\langle\cdot|$, called “bra”, denotes the conjugate transpose of the corresponding $|\cdot\rangle$.

A basis state of n multiple qubits has the form $|x_1 x_2 \dots x_n\rangle = |x_1\rangle \otimes |x_2\rangle \otimes \dots \otimes |x_n\rangle$, where \otimes is the Kronecker product and $x_i = 0$ or 1 for $i = 1, \dots, n$. The notation \otimes is usually omitted, i.e., $|x_1\rangle |x_2\rangle \dots |x_n\rangle = |x_1\rangle \otimes |x_2\rangle \otimes \dots \otimes |x_n\rangle$. For example, $|00\rangle$, $|0\rangle |0\rangle$ and $|0\rangle \otimes |0\rangle$ are the same.

The state of n multiple qubits is represented by a unit vector in \mathbb{C}^{2^n} with the form

$$|\xi\rangle = \sum_{x \in \{0,1\}^n} \alpha_x |x\rangle.$$

One important feature in quantum computing is that we cannot acquire the values of the amplitudes of a quantum state directly (Nielsen and Chuang (2011), Section 1.2). Instead, we can only acquire information from a quantum state through *measurement*. Specifically, $|x\rangle$ is obtained with probability $|\alpha_x|^2$ when $|\xi\rangle$ is measured.

A quantum state can be changed by unitary transformations. A unitary transformation on an n -qubit state can be represented by a $2^n \times 2^n$ unitary matrix. The design of useful unitary transformations is the heart of quantum computing.

2.2 Amplitude estimation based on Grover’s algorithm

The quantum amplitude estimation problem was first introduced by Brassard et al. (2002). We follow the description³ in Suzuki et al. (2020) and Grinko et al. (2021). Consider the 2^{n+1} basis states of $n + 1$ qubits. Define the basis states with the last qubit on $|1\rangle$ as *good* states and those with the last qubit on $|0\rangle$ as *bad* states. Let \mathcal{A} be a unitary transformation on $n + 1$ qubits and $|\Psi\rangle = \mathcal{A}|0\rangle_{n+1}$. Write $|\Psi\rangle$ as a linear combination of the basis states:

$$|\Psi\rangle = \sum_{x \in \{0,1\}^n} \alpha_{x,1} |x\rangle |1\rangle + \sum_{x \in \{0,1\}^n} \alpha_{x,0} |x\rangle |0\rangle.$$

When the last qubit $|\Psi\rangle$ of is measured, $|1\rangle$ is obtained with probability $\sum_{x \in \{0,1\}^n} |\alpha_{x,1}|^2$ according to the basic properties of quantum computing (Nielsen and Chuang, 2011). Let p denote this probability. The goal of amplitude estimation is to estimate p .

³The original formulation in Brassard et al. (2002) does not include the ancilla bit.

Let $|\Psi_1\rangle = (1/\sqrt{p}) \sum_{x \in \{0,1\}^n} \alpha_{x,1} |x\rangle$ and $|\Psi_0\rangle = (1/\sqrt{1-p}) \sum_{x \in \{0,1\}^n} \alpha_{x,0} |x\rangle$. $|\Psi\rangle$ can be written as

$$|\Psi\rangle = \sqrt{p} |\Psi_1\rangle |1\rangle + \sqrt{1-p} |\Psi_0\rangle |0\rangle. \quad (1)$$

In the following, $|\Psi_1\rangle |1\rangle$ and $|\Psi_0\rangle |0\rangle$ are called normalized good and bad states, respectively. Note that $|\Psi_1\rangle$ and $|\Psi_0\rangle$ are not necessarily orthogonal, and with the ancilla bit, $|\Psi_1\rangle |1\rangle$ and $|\Psi_0\rangle |0\rangle$ are orthogonal.

A special case of \mathcal{A} corresponds to querying Boolean functions through quantum oracles. Let $f : \{0,1\}^n \rightarrow \{0,1\}$ be a Boolean function. One can query f with a quantum oracle in the form of a unitary transformation \mathcal{U}_f defined as

$$\mathcal{U}_f |x\rangle |y\rangle = |x\rangle |y \oplus f(x)\rangle,$$

where $x \in \{0,1\}^n$, $y \in \{0,1\}$, and \oplus is the modulo 2 addition. The beauty of \mathcal{U}_f is that it allows quantum computers to evaluate $f(x)$ for all 2^n values of x simultaneously (Nielsen and Chuang (2011), Section 1.4.2). Let \mathcal{H} be the Hadamard transform on one qubit, that is,

$$\mathcal{H} = \frac{1}{\sqrt{2}} \begin{pmatrix} 1 & 1 \\ 1 & -1 \end{pmatrix}.$$

Let $\mathcal{H}^{\otimes n}$ be the Kronecker product of n Hadamard transforms, which changes $|0\rangle_n$ to the uniform superposition:

$$\mathcal{H}^{\otimes n} |0\rangle_n = \frac{1}{\sqrt{2^n}} \sum_{x \in \{0,1\}^n} |x\rangle.$$

One can define⁴ \mathcal{A} as $\mathcal{A} = \mathcal{U}_f(\mathcal{H}^{\otimes n} \otimes I_1)$, which has the form in (1):

$$\mathcal{A} |0\rangle_{n+1} = \sqrt{p} \frac{1}{\sqrt{\#\{x : f(x) = 1\}}} \sum_{x:f(x)=1} |x\rangle |1\rangle + \sqrt{1-p} \frac{1}{\sqrt{\#\{x : f(x) = 0\}}} \sum_{x:f(x)=0} |x\rangle |0\rangle,$$

where p is the proportion of x in $\{0,1\}^n$ such that $f(x) = 1$.

If one estimates p by classical Monte Carlo sampling, that is, sampling x_1, \dots, x_M independently and uniformly from $\{0,1\}^n$ and using $(1/M) \sum_{i=1}^M f(x_i)$ as the estimate, then the estimation error is $O(1/\sqrt{M})$. Here M equals the number of times f is queried. By contrast, the estimation error can achieve $O(1/M)$ using amplitude estimation, up to possible logarithmic factors, by querying \mathcal{U}_f through a quantum computer for M times.

We focus on amplitude estimation based on amplitude amplification (Brassard et al., 2002), an algorithm that generalizes Grover's algorithm (Grover, 1996). We follow the description in Suzuki et al. (2020). Instead of measuring $|\Psi\rangle$ directly, one can apply the following operator on $|\Psi\rangle$:

$$\mathcal{Q} = -\mathcal{A} \mathcal{S}_0 \mathcal{A}^{-1} \mathcal{S}_x,$$

⁴We follow the notation convention in the quantum computing literature, for example, Aaronson and Rall (2020): I_n is the identity matrix on n qubits, that is, a $2^n \times 2^n$ matrix.

where

$$\mathcal{S}_0 = I_{n+1} - 2|0\rangle_{n+1}\langle 0|_{n+1}, \quad \mathcal{S}_\chi = I_{n+1} - 2(I_n \otimes |1\rangle\langle 1|). \quad (2)$$

In the following, \mathcal{Q} is referred to as the Grover operator. The operator $-\mathcal{A}\mathcal{S}_0\mathcal{A}^{-1}$ performs a reflection with respect to $|\Psi\rangle$. And the operator \mathcal{S}_χ puts a negative sign to good states and does nothing to bad states, that is, $\mathcal{S}_\chi|\Psi\rangle = -\sqrt{p}|\Psi_1\rangle|1\rangle + \sqrt{1-p}|\Psi_0\rangle|0\rangle$. Also note that \mathcal{S}_χ in (2) identifies good states by simply checking whether the last qubit is on $|1\rangle$.

Let $\theta = \arcsin\sqrt{p}$, which is in $[0, \frac{\pi}{2}]$. Brassard et al. (2002) showed that applying \mathcal{Q} on $|\Psi\rangle$ for m times gives

$$\mathcal{Q}^m|\Psi\rangle = \sin((2m+1)\theta)|\Psi_1\rangle|1\rangle + \cos((2m+1)\theta)|\Psi_0\rangle|0\rangle,$$

which implies that one obtains $|1\rangle$ with probability $\sin^2((2m+1)\theta)$ when measuring the last qubit of $\mathcal{Q}^m|\Psi\rangle$. In general, one can select a sequence of m_t values for $t = 0, \dots, T$, and for each m_t take N_t independent measurements by repeating the above process for N_t times. Let X_t be the number of good states among the N_t measurements, which follows a binomial distribution:

$$\mathbb{P}(X_t = s) = \binom{N_t}{s} (\sin^2((2m_t+1)\theta))^s (\cos^2((2m_t+1)\theta))^{N_t-s}, \quad s = 0, \dots, N_t. \quad (3)$$

Define $N_{\text{oracle}} = \sum_{t=0}^T N_t m_t$, called the number of oracle queries⁵, which measures the complexity of the sample in this scenario because one needs to apply \mathcal{Q} for m_t times to obtain a single measurement. The goal is to make the estimation error for p achieve $O(1/N_{\text{oracle}})$ up to a possible logarithmic factor.

3 Main Idea

Eq. (3) is the starting point of a number of recent Grover-based amplitude estimation methods (Aaronson and Rall, 2020; Suzuki et al., 2020; Grinko et al., 2021; Nakaji, 2020), including ours.

The original motivation of applying \mathcal{Q} repeatedly is to increase the amplitude \sqrt{p} approximately linearly for small p . By contrast, a classical brute-force search algorithm increases the probability p linearly. Amplitude amplification therefore achieves a quadratic speedup over the classical brute-force search when p is small. As discovered by Aaronson and Rall (2020) and Suzuki et al. (2020), applying \mathcal{Q} repeatedly also improves the estimation of p despite that p is not necessarily small.

The estimation error based on a Monte Carlo sample of size M scales as $O(1/\sqrt{M})$. By contrast, increasing m_t in (3) in an appropriate manner can reduce the estimation error to $O(1/m_t)$. We briefly explain the reason. Let $[L, U]$ be a confidence interval for $\sin^2((2m_t+1)\theta)$ based on X_t and N_t . Due to the periodicity of $\sin^2((2m_t+1)\theta)$, such an interval is equivalent to the union of $2m_t+1$

⁵Rigorously speaking, it seems more appropriate to count the number of oracle queries in one application of \mathcal{Q} twice. Here we follow the definition in Grinko et al. (2021) for comparison.

intervals for θ :

$$\begin{aligned}
I^{+, (j)} &= \left[\frac{\arcsin \sqrt{L} + j\pi}{2m_t + 1}, \frac{\arcsin \sqrt{U} + j\pi}{2m_t + 1} \right], \quad j = 0, 1, \dots, m_t, \\
I^{-, (j)} &= \left[\frac{-\arcsin \sqrt{U} + j\pi}{2m_t + 1}, \frac{-\arcsin \sqrt{L} + j\pi}{2m_t + 1} \right], \quad j = 1, \dots, m_t.
\end{aligned} \tag{4}$$

Note that each interval is contained in one of the intervals $[0, \frac{1}{2m_t+1} \frac{\pi}{2}]$, $[\frac{1}{2m_t+1} \frac{\pi}{2}, \frac{2}{2m_t+1} \frac{\pi}{2}]$, \dots , $[\frac{2m_t}{2m_t+1} \frac{\pi}{2}, \frac{\pi}{2}]$, referred to as *period* in the following. If we are able to determine the correct period, then the estimation error for θ is in the order of $O(1/m_t)$. The estimation error for p is also in the order of $O(1/m_t)$ since $p = \sin^2(\theta)$ is Lipschitz continuous.

It is a natural idea to design a sequential algorithm to determine the period. First, use the measurements from the original $|\Psi\rangle$, i.e., $m_0 = 0$, to construct an initial confidence interval for θ , which does not have the multi-value issue. In the following steps, use the confidence interval estimated in the previous step to determine the period of θ . For simplicity, assume for now that m_t grows at a geometric rate such as $2m_t + 1 = K^t$, where K is an odd number. The number of oracle queries in the final step is therefore in the same order of that in all previous steps, both $O(K^T)$. This implies the estimation error is in the order of $O(1/N_{\text{oracle}})$. Similar ideas have appeared in the literature: although not design a sequential algorithm, Suzuki et al. (2020) recommended using an exponentially incremental sequence $\{m_t\}$ in MLAE. Grinko et al. (2021) designed a sequential algorithm that uses data-dependent $\{m_t\}$ determined by a search sub-routine, which will be discussed in Section 5. Our choice of $\{m_t\}$ will be given in Section 4.

Although promising, the above idea has a serious caveat: when the true value of θ is at or near the boundary of two adjacent periods for the subsequent step, the estimated confidence interval can overlap with both periods even though we are able to control the length of the interval. Panel (a) in Figure 1 illustrates this problem. The true value of p is set as 0.2 in this toy example. The confidence interval for θ from step 0 overlaps with two periods $[0, \pi/6]$ and $[\pi/6, \pi/3]$, which brings difficulty in step 1: the algorithm does not know how to choose between the two intervals, each contained in a period. We propose the following solution to the problem, which is the key ingredient of our algorithm.

Denote the confidence interval for θ in step t by $[\theta_t^L, \theta_t^U]$. If there exists k such that $\frac{k}{2m_{t+1}+1} \frac{\pi}{2} \in (\theta_t^L, \theta_t^U)$, then we introduce an adjustment factor

$$r_{t+1} = \sin^2 \left(\frac{k}{2m_{t+1} + 1} \frac{\pi}{2} \right) / \sin^2(\theta_t^U);$$

otherwise $r_{t+1} = 1$. The factor r_{t+1} adjusts the scale of θ and makes the new confidence interval contained in a single period of length $\frac{1}{2m_{t+1}+1} \frac{\pi}{2}$. Specifically, let $\theta_{t+1} = \arcsin \sqrt{r_{t+1}p}$. It is easy to check that the upper limit of the confidence interval for θ_{t+1} is $\frac{k}{2m_{t+1}+1} \frac{\pi}{2}$ according to the definition of r_{t+1} . We will prove in Lemma 1 that the confidence interval contracts with this adjustment, which implies that the interval for θ_{t+1} is fully contained in $[\frac{k-1}{2m_{t+1}+1} \frac{\pi}{2}, \frac{k}{2m_{t+1}+1} \frac{\pi}{2}]$ when we control the length of $[\theta_t^L, \theta_t^U]$ within $\frac{1}{2m_{t+1}+1} \frac{\pi}{2}$.

In step $t+1$, we add a qubit and define an adjusted unitary transformation on $n+2$ qubits such that the probability of obtaining a good state is $r_{t+1}p$ when measuring the state after the transformation.

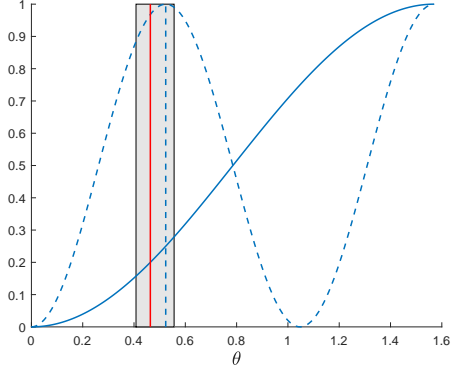
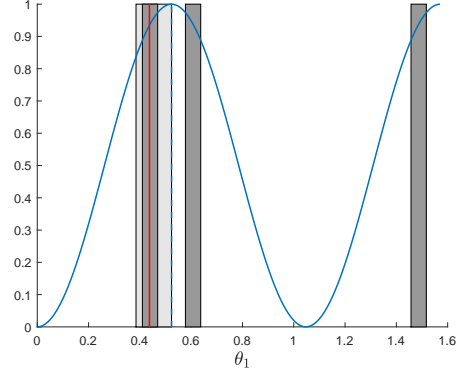
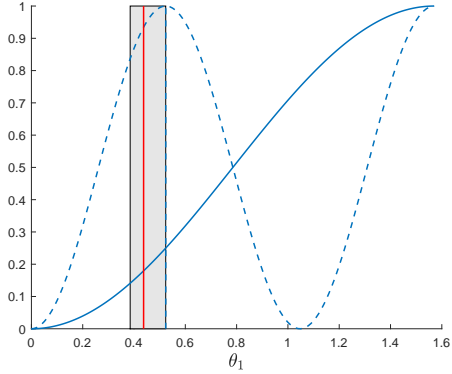
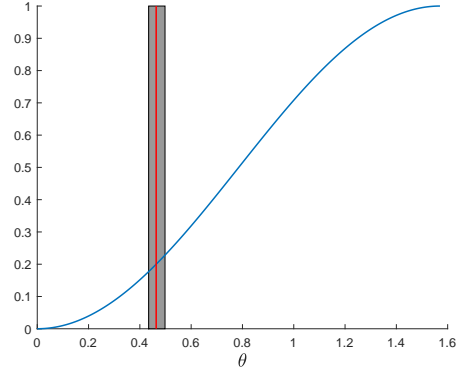
(a) Confidence interval for θ in step 0(c) Confidence interval for θ_1 in step 1(b) Confidence interval for θ_1 in step 0(d) Confidence interval for θ in step 1

Figure 1: An illustration of the first two steps of the adaptive algorithm. Panel (a): the confidence interval for θ in step 0 overlaps with two periods $[0, \frac{\pi}{6}]$ and $[\frac{\pi}{6}, \frac{\pi}{3}]$. Panel (b): the upper limit of the confidence interval for $\theta_1 = \arcsin \sqrt{r_1 \sin^2(\theta)}$ coincides with the boundary so that the interval is contained in the period $[0, \frac{\pi}{6}]$. Panel (c): the confidence interval for θ_1 in step 1, constructed by running the Grover operator (6) on $(\mathcal{A} \otimes \mathcal{R}_{t+1}) |0\rangle_{n+1} |0\rangle$. Panel (d): convert to the confidence interval for θ .

Such an adjustment has been introduced in Aaronson and Rall (2020) for a different purpose. Let \mathcal{R}_{t+1} satisfy $\mathcal{R}_{t+1}|0\rangle = \sqrt{r_{t+1}}|1\rangle + \sqrt{1-r_{t+1}}|0\rangle$. Then

$$\begin{aligned} |\tilde{\Psi}\rangle = (\mathcal{A} \otimes \mathcal{R}_{t+1})|0\rangle_{n+1}|0\rangle &= \sqrt{r_{t+1}p}|\Psi_1\rangle|1\rangle|1\rangle + \sqrt{r_{t+1}(1-p)}|\Psi_0\rangle|0\rangle|1\rangle \\ &+ \sqrt{(1-r_{t+1})p}|\Psi_1\rangle|1\rangle|0\rangle + \sqrt{(1-r_{t+1})(1-p)}|\Psi_0\rangle|0\rangle|0\rangle. \end{aligned} \quad (5)$$

Now a basis state is defined as good state if the last two qubits are on $|11\rangle$.

Remark A quantum state can be viewed as a random variable when it is measured. Using the terminology of probability, the above operation is adding a “random variable” $\mathcal{R}_{t+1}|0\rangle$, which equals 1 with probability r_{t+1} . From (5), $|\Psi\rangle$ and $\mathcal{R}_{t+1}|0\rangle$ can be understood as “independent random variables”. The “joint probability” of both $\mathcal{R}_{t+1}|0\rangle$ and the last bit of $|\Psi\rangle$ being 1 is therefore $r_{t+1}p$. Below we give details of the Grover operator on $|\Psi\rangle \otimes \mathcal{R}_{t+1}|0\rangle$. The readers who are only interested in the statistical model can directly go to (8).

Note that the last three terms in (5) are orthogonal to $|\Psi_111\rangle$. Denote the combination of these terms, after normalization, by $|\Psi_111^\perp\rangle$. We define an operator that amplifies the amplitude $\sqrt{r_{t+1}p}$:

$$\mathcal{Q}_{t+1} = -(\mathcal{A} \otimes \mathcal{R}_{t+1})(I_{n+2} - 2|0\rangle_{n+2}\langle 0|_{n+2})(\mathcal{A} \otimes \mathcal{R}_{t+1})^{-1}(I_{n+2} - 2(I_n \otimes |11\rangle\langle 11|)). \quad (6)$$

In (6), the operator $I_{n+2} - 2(I_n \otimes |11\rangle\langle 11|)$ puts a negative sign to $|\Psi_111\rangle$ and does nothing to other terms. That is,

$$(I_{n+2} - 2(I_n \otimes |11\rangle\langle 11|))|\Phi\rangle = -\sqrt{r_{t+1}p}|\Psi_111\rangle + \sqrt{1-r_{t+1}p}|\Psi_111^\perp\rangle.$$

The operator $-(\mathcal{A} \otimes \mathcal{R}_{t+1})(I_{n+2} - 2|0\rangle_{n+2}\langle 0|_{n+2})(\mathcal{A} \otimes \mathcal{R}_{t+1})^{-1} = -(I_{n+2} - 2|\tilde{\Psi}\rangle\langle \tilde{\Psi}|)$ performs a reflection with respect to $\tilde{\Psi}$. Therefore, by the same argument in Brassard et al. (2002),

$$\mathcal{Q}_{t+1}^{m_{t+1}}|\tilde{\Psi}\rangle = \sin((2m_{t+1} + 1)\theta_{t+1})|\Psi_111\rangle + \cos((2m_{t+1} + 1)\theta_{t+1})|\Psi_111^\perp\rangle. \quad (7)$$

When repeating the process and measuring $\mathcal{Q}_{t+1}^{m_{t+1}}|\tilde{\Psi}\rangle$ for N_{t+1} times, the number of observed good states X_{t+1} follows a binomial distribution:

$$\mathbb{P}(X_{t+1} = s) = \binom{N_{t+1}}{s} (\sin^2((2m_{t+1} + 1)\theta_{t+1}))^s (\cos^2((2m_{t+1} + 1)\theta_{t+1}))^{N_{t+1}-s}, \quad s = 0, \dots, N_{t+1}. \quad (8)$$

Since θ_{t+1} is contained in $[\frac{k-1}{2m_{t+1}+1}\frac{\pi}{2}, \frac{k}{2m_{t+1}+1}\frac{\pi}{2}]$ for certain k , only one interval with the form in (4) is a legitimate confidence interval for θ_{t+1} . Finally, we convert the interval for θ_{t+1} back to the interval for θ . Denote the new interval for θ by $[\theta_{t+1}^L, \theta_{t+1}^U]$. At the same time, we select appropriate N_{t+1} such that $|\theta_{t+1}^L - \theta_{t+1}^U| \leq \frac{1}{2m_{t+2}+1}\frac{\pi}{2}$ so that the recursion can continue. We illustrate the first two steps of the above procedure in Figure 1.

We apply (5) and (6) in a different way than Aaronson and Rall (2020). In their method, \mathcal{R} is defined as $\mathcal{R}|0\rangle = \frac{1}{1000}|1\rangle + \sqrt{1 - \frac{1}{1000^2}}|0\rangle$, which shrinks p by a factor of 10^{-6} . By contrast, we adjust r_t adaptively to avoid the period ambiguity in each step. In practice, r_t is typical close to 1, which makes the estimation lose very little efficiency due to the adjustment.

4 Algorithm

We formally describe the adaptive algorithm in Algorithm 1. Without loss of generality, we assume $p \in [0, \frac{1}{2}]$ because otherwise one can add artificial bad states to the system by adding a qubit on $\frac{1}{\sqrt{2}}|1\rangle + \frac{1}{\sqrt{2}}|0\rangle$ at the beginning of the algorithm. We need such an assumption to control the length of the confidence interval when we convert the interval for θ_t back to the interval for θ (Panel (d) in Figure 1). See lines 17–19 in Algorithm 1 and Lemma 2 for details.

We choose $\{m_t\}$ that grows at least as fast as a geometric progression. That is, we choose m_{t+1} as the largest integer such that $|\theta_t^L - \theta_t^U| \leq \frac{1}{2m_{t+1}+1} \frac{\pi}{2}$ (lines 20 and 24 in Algorithm 1), which implies $2m_{t+1} + 1 \geq K^t$. This choice takes full advantage of the precision of the current interval for θ and can potentially make the length of the interval reach the desired precision level ϵ in fewer steps.

Another ingredient of Algorithm 1 is that instead of preselecting the sample size N_t in step t such that $|\theta_t^L - \theta_t^U| \leq \frac{1}{K} \frac{1}{2m_t+1} \frac{\pi}{2}$, which is usually very conservative, we gradually increase N_t by a fixed N_{shots} at each time until $|\theta_t^L - \theta_t^U| \leq \frac{1}{K} \frac{1}{2m_t+1} \frac{\pi}{2}$ is satisfied. This brings a subtle difficulty to the theoretical analysis. That is, when the condition $|\theta_t^L - \theta_t^U| \leq \frac{1}{K} \frac{1}{2m_t+1} \frac{\pi}{2}$ is met, the data used to construct the confidence interval $[L_t, U_t]$ for $\sin^2((2m_t + 1)\theta_t)$ (line 10 in Algorithm 1), rigorously speaking, is no longer a random sample. More specifically,

$$\mathbb{P}\left(X_t = j \mid |\theta_t^L - \theta_t^U| \leq \frac{1}{K} \frac{1}{2m_t+1} \frac{\pi}{2}\right) \neq \binom{N_t}{j} (\sin^2((2m_t + 1)\theta_t))^j (\cos^2((2m_t + 1)\theta_t))^{N_t-j},$$

so Hoeffding's inequality (Hoeffding, 1963) cannot be directly applied to interval estimation. To resolve this difficulty, we choose δ_t (line 9 in Algorithm 1) such that an infinite sequence of confidence intervals based on jN_{shots} ($j = 1, 2, \dots$) observations *simultaneously* contain $\sin^2((2m_t + 1)\theta_t)$ with probability at least $1 - \frac{\alpha}{T+1}$. Therefore, the interval satisfying $|\theta_t^L - \theta_t^U| \leq \frac{1}{K} \frac{1}{2m_t+1} \frac{\pi}{2}$ also contains $\sin^2((2m_t + 1)\theta_t)$ with probability at least $1 - \frac{\alpha}{T+1}$.

Next, we present the main theorem showing that the output $[p^L, p^U]$ of Algorithm 1 reaches the pre-specified confidence level $1 - \alpha$ and precision level ϵ . Moreover, the number of oracle queries N_{oracle} achieves $O(1/\epsilon)$ up to a double-logarithmic factor of ϵ .

Theorem 1. *If $0 \leq p \leq 1/2$, the output $[p^L, p^U]$ of Algorithm 1 satisfies the following properties:*

1. $\mathbb{P}(p \in [p^L, p^U]) \geq 1 - \alpha$.
2. $|p^L - p^U| \leq \epsilon$.
- 3.

$$N_{\text{oracle}} = O\left(\log\left(\frac{\pi^2(T+1)}{3\alpha}\right) \frac{1}{\epsilon}\right),$$

where $T = \lceil \log \frac{\pi}{K\epsilon} / \log K \rceil$.

Proof. Proof of Claim 1: Let $\theta = \arcsin \sqrt{p}$, $\theta_t = \arcsin \sqrt{r_t p}$, $t = 0, \dots, T$. We first show that

$$\mathbb{P}(\sin^2((2m_t + 1)\theta_t) \in [L_t, U_t], t = 0, \dots, T) \geq 1 - \alpha.$$

Algorithm 1: Adaptive Algorithm for Amplitude Estimation

Input: $\epsilon, \alpha, K, N_{\text{shots}}$ // ϵ : precision level; $1 - \alpha$: confidence level; K : odd number ≥ 3

- 1 $T \leftarrow \lceil \log \frac{\pi}{K\epsilon} / \log K \rceil, r_0 \leftarrow 1, \hat{k}_0 \leftarrow 0, m_0 \leftarrow 0$ // T : upper bound of the number of iterations
- 2 **for** $t = 0$ **to** T **do**
- 3 add artificial bad states as (5) such that $\mathbb{P}(\text{good state}) = r_t p$
- 4 $X_t \leftarrow 0, j \leftarrow 0$
- 5 **repeat**
- 6 // increase the sample size N_t by N_{shots} at each time until the length of the CI for θ is less than or equal to $\frac{1}{K} \frac{1}{2m_t+1} \frac{\pi}{2}$
- 7 $j \leftarrow j + 1$
- 8 $N_t \leftarrow j N_{\text{shots}}$
- 9 $X_t \leftarrow X_t +$ the number of good states observed by measuring $Q_t^{m_t} |\tilde{\Psi}\rangle$ (defined in (7)) for N_{shots} times
- 10 $\delta_t \leftarrow \sqrt{\log \left(\frac{\pi^2(T+1)}{3\alpha} j^2 \right)} \frac{1}{2N_t}$ // the choice of δ_t makes the coverage probability at least $1 - \frac{\alpha}{T+1}$ in step t
- 11 $L_t \leftarrow \max \left(\frac{X_t}{N_t} - \delta_t, 0 \right), U_t \leftarrow \min \left(\frac{X_t}{N_t} + \delta_t, 1 \right)$
- 12 **if** $\hat{k}_t \equiv 0 \pmod{2}$ // CI for θ_t , based on the period estimated from step $t - 1$
- 13 **then**
- 14 $[\theta_t^L, \theta_t^U] \leftarrow \left[\frac{\arcsin \sqrt{L_t + \hat{k}_t \pi / 2}}{2m_t + 1}, \frac{\arcsin \sqrt{U_t + \hat{k}_t \pi / 2}}{2m_t + 1} \right]$
- 15 **else**
- 16 $[\theta_t^L, \theta_t^U] \leftarrow \left[\frac{-\arcsin \sqrt{U_t + (\hat{k}_t + 1) \pi / 2}}{2m_t + 1}, \frac{-\arcsin \sqrt{L_t + (\hat{k}_t + 1) \pi / 2}}{2m_t + 1} \right]$
- 17 **end**
- 18 $\theta_t^L \leftarrow \min(\theta_t^L, \arcsin \sqrt{r_t / 2}), \theta_t^U \leftarrow \min(\theta_t^U, \arcsin \sqrt{r_t / 2})$
- 19 **if** $r_t < 1$ **then**
- 20 $[\theta_t^L, \theta_t^U] \leftarrow \left[\arcsin \sqrt{(\sin \theta_t^L)^2 / r_t}, \arcsin \sqrt{(\sin \theta_t^U)^2 / r_t} \right]$ // CI for θ
- 21 **until** $|\theta_t^L - \theta_t^U| \leq \frac{1}{K} \frac{1}{2m_t + 1} \frac{\pi}{2};$
- 22 $p^L \leftarrow \sin^2(\theta_t^L), p^U \leftarrow \sin^2(\theta_t^U)$
- 23 **if** $t = T$ **OR** $|p^L - p^U| \leq \epsilon$ **then**
- 24 go to **Output**
- 25 $m_{t+1} \leftarrow \lfloor \frac{1}{|\theta_t^L - \theta_t^U|} \frac{\pi}{4} - \frac{1}{2} \rfloor$
- 26 $\hat{k}_{t+1} \leftarrow \lfloor 2(2m_{t+1} + 1)\theta_t^L / \pi \rfloor$ // determine the period
- 27 **if** $\frac{\hat{k}_{t+1} + 1}{2m_{t+1} + 1} \frac{\pi}{2} < \theta_t^U$ **then**
- 28 $r_{t+1} \leftarrow \sin^2 \left(\frac{\hat{k}_{t+1} + 1}{2m_{t+1} + 1} \frac{\pi}{2} \right) / \sin^2(\theta_t^U)$ // set the adjustment factor r_{t+1} if (θ_t^L, θ_t^U) contains a boundary point of two periods
- 29 **else**
- 30 $r_{t+1} \leftarrow 1$
- 31 **end**
- 32 **end**

Output: $[p^L, p^U]$

Let $Z_{t,1}, Z_{t,2}, \dots$ be a sequence of independently and identically distributed random variables from $\text{Ber}(\sin^2((2m_t + 1)\theta_t))$. For $j = 1, 2, \dots$, let

$$\eta_j = \sqrt{\log\left(\frac{\pi^2(T+1)}{3\alpha}j^2\right) \frac{1}{2jN_{\text{shots}}}}.$$

From Hoeffding's inequality, for all j ,

$$\begin{aligned} \mathbb{P}\left(\left|\frac{1}{jN_{\text{shots}}}\sum_{i=1}^{jN_{\text{shots}}}Z_{t,i} - \sin^2((2m_t + 1)\theta_t)\right| \geq \eta_j \middle| m_t, r_t\right) &\leq 2\exp(-2jN_{\text{shots}}\eta_j^2) = \frac{\alpha}{T+1} \frac{6}{\pi^2} \frac{1}{j^2}, \\ \mathbb{P}\left(\exists j \in \{1, 2, \dots\} \text{ s.t. } \left|\frac{1}{jN_{\text{shots}}}\sum_{i=1}^{jN_{\text{shots}}}Z_{t,i} - \sin^2((2m_t + 1)\theta_t)\right| \geq \eta_j \middle| m_t, r_t\right) &\leq \frac{\alpha}{T+1} \sum_{j=1}^{\infty} \frac{6}{\pi^2} \frac{1}{j^2} = \frac{\alpha}{T+1}. \end{aligned} \quad (9)$$

Let \hat{J}_t be the smallest integer in step t such that $|\theta_t^L - \theta_t^U| \leq \frac{1}{K} \frac{1}{2m_t + 1} \frac{\pi}{2}$, and let $N_t = \hat{J}_t N_{\text{shots}}$, $\delta_t = \eta_{\hat{J}_t}$ (the **repeat** loop in Algorithm 1). We will leave until the proof of Claim 3 to show there is an upper bound for \hat{J}_t . Eq. (9) implies

$$\mathbb{P}\left(\left|\frac{1}{N_t}\sum_{i=1}^{N_t}Z_{t,i} - \sin^2((2m_t + 1)\theta_t)\right| \geq \delta_t \middle| m_t, r_t\right) \leq \frac{\alpha}{T+1},$$

and

$$\mathbb{P}\left(\left|\frac{1}{N_t}\sum_{i=1}^{N_t}Z_{t,i} - \sin^2((2m_t + 1)\theta_t)\right| \geq \delta_t\right) \leq \frac{\alpha}{T+1}.$$

Therefore,

$$\mathbb{P}\left(\sin^2((2m_t + 1)\theta_t) \in [L_t, U_t], t = 0, \dots, T\right) \geq 1 - \alpha.$$

Let \hat{T} be the stopping time of t in the algorithm. The above inequality implies

$$\mathbb{P}\left(\sin^2((2m_t + 1)\theta_t) \in [L_t, U_t], t = 0, \dots, \hat{T}\right) \geq 1 - \alpha.$$

Next we show that

$$\sin^2((2m_t + 1)\theta_t) \in [L_t, U_t], t = 0, \dots, \hat{T} \quad (*)$$

implies $p \in [p^L, p^U]$, which proves Claim 1. For the rest of the proof of Claim 1, we assume (*).

We first show that for $t = 0, \dots, \hat{T}$, θ_t belongs to the interval defined by (lines 11–16 in Algorithm 1):

$$\begin{aligned} &\left[\frac{\arcsin\sqrt{L_t} + \hat{k}_t\pi/2}{2m_t + 1}, \frac{\arcsin\sqrt{U_t} + \hat{k}_t\pi/2}{2m_t + 1}\right], \text{ if } \hat{k}_t \text{ is even,} \\ &\left[\frac{-\arcsin\sqrt{U_t} + (\hat{k}_t + 1)\pi/2}{2m_t + 1}, \frac{-\arcsin\sqrt{L_t} + (\hat{k}_t + 1)\pi/2}{2m_t + 1}\right], \text{ otherwise.} \end{aligned}$$

Denote the interval by $[\check{\theta}_t^L, \check{\theta}_t^U]$.

We use induction. The conclusion holds for $t = 0$ because $\theta = \theta_0 \in [\arcsin \sqrt{L_0}, \arcsin \sqrt{U_0}]$, which is a single interval corresponding to $\hat{k}_0 = 0$. Assume the conclusion holds for step t . We now consider step $t + 1$. Let (lines 17–19)

$$\begin{aligned}\theta_t^L &= \arcsin \sqrt{\sin^2(\min(\check{\theta}_t^L, \arcsin \sqrt{r_t/2}))/r_t} = \min \left(\arcsin \sqrt{\sin^2(\check{\theta}_t^L)/r_t}, \pi/4 \right), \\ \theta_t^U &= \arcsin \sqrt{\sin^2(\min(\check{\theta}_t^U, \arcsin \sqrt{r_t/2}))/r_t} = \min \left(\arcsin \sqrt{\sin^2(\check{\theta}_t^U)/r_t}, \pi/4 \right).\end{aligned}$$

Note that

$$\theta_t \in [\check{\theta}_t^L, \check{\theta}_t^U] \Rightarrow \theta \in \left[\arcsin \sqrt{\sin^2(\check{\theta}_t^L)/r_t}, \arcsin \sqrt{\sin^2(\check{\theta}_t^U)/r_t} \right],$$

which further implies $\theta \in [\theta_t^L, \theta_t^U]$ since $p \leq 1/2$.

Consider intervals $[0, \frac{1}{2m_{t+1}+1} \frac{\pi}{2}]$, $[\frac{1}{2m_{t+1}+1} \frac{\pi}{2}, \frac{2}{2m_{t+1}+1} \frac{\pi}{2}]$, \dots , $[\frac{2m_{t+1}}{2m_{t+1}+1} \frac{\pi}{2}, \frac{\pi}{2}]$. The choice of \hat{k}_{t+1} (line 25) makes $\frac{\hat{k}_{t+1}}{2m_{t+1}+1} \frac{\pi}{2} \leq \theta_t^L < \frac{\hat{k}_{t+1}+1}{2m_{t+1}+1} \frac{\pi}{2}$. If $\theta_t^U \leq \frac{\hat{k}_{t+1}+1}{2m_{t+1}+1} \frac{\pi}{2}$,

$$[\theta_t^L, \theta_t^U] \subset \left[\frac{\hat{k}_{t+1}}{2m_{t+1}+1} \frac{\pi}{2}, \frac{\hat{k}_{t+1}+1}{2m_{t+1}+1} \frac{\pi}{2} \right].$$

Otherwise, define

$$r_{t+1} = \sin^2 \left(\frac{\hat{k}_{t+1}+1}{2m_{t+1}+1} \frac{\pi}{2} \right) / \sin^2(\theta_t^U),$$

which implies $\arcsin \sqrt{r_{t+1}(\sin \theta_t^U)^2} = \frac{\hat{k}_{t+1}+1}{2m_{t+1}+1} \frac{\pi}{2}$.

From Lemma 1 in the appendix, since $r_{t+1} \leq 1$,

$$\left| \arcsin \sqrt{r_{t+1}(\sin \theta_t^L)^2} - \arcsin \sqrt{r_{t+1}(\sin \theta_t^U)^2} \right| \leq |\theta_t^L - \theta_t^U| \leq \frac{1}{2m_{t+1}+1} \frac{\pi}{2},$$

where the last inequality is guaranteed by the algorithm (line 20). Therefore,

$$\left[\arcsin \sqrt{r_{t+1}(\sin \theta_t^L)^2}, \arcsin \sqrt{r_{t+1}(\sin \theta_t^U)^2} \right] \subset \left[\frac{\hat{k}_{t+1}}{2m_{t+1}+1} \frac{\pi}{2}, \frac{\hat{k}_{t+1}+1}{2m_{t+1}+1} \frac{\pi}{2} \right].$$

Therefore,

$$\begin{aligned}\theta \in [\theta_t^L, \theta_t^U] &\Rightarrow \theta_{t+1} \in \left[\arcsin \sqrt{r_{t+1}(\sin \theta_t^L)^2}, \arcsin \sqrt{r_{t+1}(\sin \theta_t^U)^2} \right] \\ &\Rightarrow \theta_{t+1} \in \left[\frac{\hat{k}_{t+1}}{2m_{t+1}+1} \frac{\pi}{2}, \frac{\hat{k}_{t+1}+1}{2m_{t+1}+1} \frac{\pi}{2} \right].\end{aligned}$$

Note that $\sin^2((2m_{t+1}+1)\phi) = \frac{1}{2} - \frac{1}{2} \cos(2(2m_{t+1}+1)\phi)$ is strictly increasing for all $\phi \in \left[\frac{\hat{k}_{t+1}}{2m_{t+1}+1} \frac{\pi}{2}, \frac{\hat{k}_{t+1}+1}{2m_{t+1}+1} \frac{\pi}{2} \right]$ when \hat{k}_{t+1} is even, and is strictly decreasing in that interval when \hat{k}_{t+1} is odd. When \hat{k}_{t+1} is even, the unique solution of equation $\sin^2((2m_{t+1}+1)\phi) = y$ in $\left[\frac{\hat{k}_{t+1}}{2m_{t+1}+1} \frac{\pi}{2}, \frac{\hat{k}_{t+1}+1}{2m_{t+1}+1} \frac{\pi}{2} \right]$ is

$$\phi = \frac{\arcsin \sqrt{y}}{2m_{t+1}+1} + \frac{\hat{k}_{t+1}}{2m_{t+1}+1} \frac{\pi}{2}. \quad (10)$$

In fact, one can verify that (10) satisfies the equation and is within $\left[\frac{\hat{k}_{t+1}}{2m_{t+1}+1} \frac{\pi}{2}, \frac{\hat{k}_{t+1}+1}{2m_{t+1}+1} \frac{\pi}{2} \right]$. The solution is unique because the function is strictly monotonic. Therefore, the function $y = \sin^2((2m_{t+1}+1)\phi)$ has an inverse on $\left[\frac{\hat{k}_{t+1}}{2m_{t+1}+1} \frac{\pi}{2}, \frac{\hat{k}_{t+1}+1}{2m_{t+1}+1} \frac{\pi}{2} \right]$, defined by (10). Furthermore, since the function is increasing,

$$\begin{aligned} \theta_{k+1} &\in \left[\frac{\hat{k}_{t+1}}{2m_{t+1}+1} \frac{\pi}{2}, \frac{\hat{k}_{t+1}+1}{2m_{t+1}+1} \frac{\pi}{2} \right] \text{ and } \sin^2((2m_{t+1}+1)\theta_{t+1}) \in [L_{t+1}, U_{t+1}] \\ \Leftrightarrow \theta_{k+1} &\in \left[\frac{\arcsin \sqrt{L_{t+1}} + \hat{k}_{t+1}\pi/2}{2m_{t+1}+1}, \frac{\arcsin \sqrt{U_{t+1}} + \hat{k}_{t+1}\pi/2}{2m_{t+1}+1} \right]. \end{aligned}$$

Similarly, when \hat{k}_{t+1} is odd,

$$\begin{aligned} \theta_{k+1} &\in \left[\frac{\hat{k}_{t+1}}{2m_{t+1}+1} \frac{\pi}{2}, \frac{\hat{k}_{t+1}+1}{2m_{t+1}+1} \frac{\pi}{2} \right] \text{ and } \sin^2((2m_{t+1}+1)\theta_{t+1}) \in [L_{t+1}, U_{t+1}] \\ \Leftrightarrow \theta_{k+1} &\in \left[\frac{-\arcsin \sqrt{U_{t+1}} + (\hat{k}_{t+1}+1)\pi/2}{2m_{t+1}+1}, \frac{-\arcsin \sqrt{L_{t+1}} + (\hat{k}_{t+1}+1)\pi/2}{2m_{t+1}+1} \right]. \end{aligned}$$

We have therefore proved the conclusion for $t+1$. Moreover, we have also shown that $\theta \in [\theta_t^L, \theta_t^U]$ in the above proof. Finally, by the definition of $[p^L, p^U]$, $p \in [p^L, p^U]$.

Proof of Claim 2: We only need to show that the claim holds if the algorithm stops at step T because otherwise it automatically holds (line 22). Since m_{t+1} is the largest integer such that $|\theta_t^L - \theta_t^U| \leq \frac{1}{2m_{t+1}+1} \frac{\pi}{2}$ (line 24) and the algorithm requires $|\theta_t^L - \theta_t^U| \leq \frac{1}{K} \frac{1}{2m_t+1} \frac{\pi}{2}$, we have $2m_{t+1}+1 \geq K(2m_t+1)$. A simple induction argument shows $2m_t+1 \geq K^t$ for $t = 0, \dots, T$. Since

$$T = \left\lceil \log \frac{\pi}{K\epsilon} / \log K \right\rceil,$$

we have

$$\begin{aligned} |\theta_T^L - \theta_T^U| &\leq \frac{1}{K} \frac{1}{2m_t+1} \frac{\pi}{2} \leq \frac{1}{K^{T+1}} \frac{\pi}{2}, \\ |p^L - p^U| &= |(\sin \theta_T^L)^2 - (\sin \theta_T^U)^2| \leq 2|\theta_T^L - \theta_T^U| \leq \frac{\pi}{K^{T+1}} \leq \epsilon. \end{aligned}$$

Proof of Claim 3: We first show that \hat{J}_t has an upper bound. That is, if

$$j = \max \left(\left\lceil \frac{4}{c_t^2 N_{\text{shots}}} \log \left(\frac{\pi^2(T+1)}{3\alpha} \right) \right\rceil, \left\lceil \frac{64}{c_t^4 N_{\text{shots}}^2} \right\rceil \right),$$

where $c_t = \sin^2\left(\sqrt{\frac{r_t}{2}} \frac{1}{K} \frac{\pi}{2}\right)$, and $N_t = jN_{\text{shots}}$, $\delta_t = \eta_j$, then we will show $|\theta_t^L - \theta_t^U| \leq \frac{1}{K} \frac{1}{2m_t+1} \frac{\pi}{2}$. Recall that (line 9)

$$\delta_t = \sqrt{\log\left(\frac{\pi^2(T+1)}{3\alpha} j^2\right) \frac{1}{2jN_{\text{shots}}}}.$$

It follows that

$$\begin{aligned} \delta_t &= \sqrt{\left(\log\left(\frac{\pi^2(T+1)}{3\alpha}\right) + 2\log j\right) \frac{1}{2jN_{\text{shots}}}} \\ &\leq \sqrt{\left(\log\left(\frac{\pi^2(T+1)}{3\alpha}\right) + 2\sqrt{j}\right) \frac{1}{2jN_{\text{shots}}}} \\ &\leq \sqrt{2 \max\left(\log\left(\frac{\pi^2(T+1)}{3\alpha}\right) \frac{1}{2jN_{\text{shots}}}, 2\sqrt{j} \frac{1}{2jN_{\text{shots}}}\right)} \\ &\leq \frac{1}{2} \sin^2\left(\sqrt{\frac{r_t}{2}} \frac{1}{K} \frac{\pi}{2}\right). \end{aligned}$$

From Lemma 3,

$$\begin{aligned} \left|\arcsin \sqrt{L_t} - \arcsin \sqrt{U_t}\right| &\leq \arcsin \sqrt{|L_t - U_t|} \leq \arcsin \sqrt{2\delta_t} \leq \sqrt{\frac{r_t}{2}} \frac{1}{K} \frac{\pi}{2} \\ \Rightarrow |\check{\theta}_t^L - \check{\theta}_t^U| &= \frac{1}{2m_t+1} \left|\arcsin \sqrt{L_t} - \arcsin \sqrt{U_t}\right| \leq \sqrt{\frac{r_t}{2}} \frac{1}{K} \frac{1}{2m_t+1} \frac{\pi}{2} \\ \Rightarrow \left|\min\left(\check{\theta}_t^L, \arcsin \sqrt{r_t/2}\right) - \min\left(\check{\theta}_t^U, \arcsin \sqrt{r_t/2}\right)\right| &\leq \sqrt{\frac{r_t}{2}} \frac{1}{K} \frac{1}{2m_t+1} \frac{\pi}{2}. \end{aligned}$$

From Lemma 2,

$$\begin{aligned} |\theta_t^L - \theta_t^U| &= \left|\arcsin \sqrt{\sin^2\left(\min\left(\check{\theta}_t^L, \arcsin \sqrt{r_t/2}\right)\right) / r_t} - \arcsin \sqrt{\sin^2\left(\min\left(\check{\theta}_t^U, \arcsin \sqrt{r_t/2}\right)\right) / r_t}\right| \\ &\leq \sqrt{\frac{2}{r_t}} \left|\min\left(\check{\theta}_t^L, \arcsin \sqrt{r_t/2}\right) - \min\left(\check{\theta}_t^U, \arcsin \sqrt{r_t/2}\right)\right| \leq \frac{1}{K} \frac{1}{2m_t+1} \frac{\pi}{2}. \end{aligned}$$

We now give a bound for $1/r_t$. When $r_t < 1$,

$$\begin{aligned} r_t &= \sin^2\left(\frac{\hat{k}_t+1}{2m_t+1} \frac{\pi}{2}\right) \Big/ \sin^2(\theta_{t-1}^U) \\ \Rightarrow \frac{1}{r_t} &= \frac{\sin^2(\theta_{t-1}^U)}{\sin^2\left(\frac{\hat{k}_t+1}{2m_t+1} \frac{\pi}{2}\right)} \leq \frac{\sin^2\left(\frac{\hat{k}_t+2}{2m_t+1} \frac{\pi}{2}\right)}{\sin^2\left(\frac{\hat{k}_t+1}{2m_t+1} \frac{\pi}{2}\right)} \leq \frac{\sin^2\left(\frac{\hat{k}_t+2}{2m_t+1} \frac{\pi}{2}\right)}{\sin^2\left(\frac{\hat{k}_t/2+1}{2m_t+1} \frac{\pi}{2}\right)} = \left(2 \cos\left(\frac{\hat{k}_t/2+1}{2m_t+1} \frac{\pi}{2}\right)\right)^2 \leq 4. \quad (11) \end{aligned}$$

Therefore,

$$N_t = O\left(\log\left(\frac{\pi^2(T+1)}{3\alpha}\right)\right).$$

We now bound N_{oracle} . Since \hat{T} is the smallest number such that $|(\sin \theta_{\hat{T}}^L)^2 - (\sin \theta_{\hat{T}}^U)^2| \leq \epsilon$, $|(\sin \theta_{\hat{T}-1}^L)^2 - (\sin \theta_{\hat{T}-1}^U)^2| \geq \epsilon$. And recall $|\theta_{\hat{T}-1}^L - \theta_{\hat{T}-1}^U| \leq \frac{1}{2m_{\hat{T}+1}} \frac{\pi}{2}$, which gives

$$\epsilon \leq |(\sin \theta_{\hat{T}-1}^L)^2 - (\sin \theta_{\hat{T}-1}^U)^2| \leq 2|\theta_{\hat{T}-1}^L - \theta_{\hat{T}-1}^U| \leq \frac{\pi}{2m_{\hat{T}+1}} \Rightarrow 2m_{\hat{T}+1} \leq \frac{\pi}{\epsilon}.$$

And since $2m_{t+1} + 1 \geq K(2m_t + 1)$, a simple induction argument shows

$$2m_t + 1 \leq \frac{1}{K^{\hat{T}-t}} \frac{\pi}{\epsilon}, \quad t = 0, \dots, \hat{T}.$$

Finally,

$$\begin{aligned} N_{\text{oracle}} &= \sum_{t=0}^{\hat{T}} N_t m_t \leq O\left(\log\left(\frac{\pi^2(T+1)}{3\alpha}\right)\right) \sum_{t=0}^{\hat{T}} (2m_t + 1) \leq O\left(\log\left(\frac{\pi^2(T+1)}{3\alpha}\right)\right) \frac{\pi}{\epsilon} \sum_{t=0}^{\hat{T}} \frac{1}{K^t} \\ &\leq O\left(\log\left(\frac{\pi^2(T+1)}{3\alpha}\right)\right) \frac{\pi}{\epsilon} \sum_{t=0}^{\infty} \frac{1}{K^t} = O\left(\log\left(\frac{\pi^2(T+1)}{3\alpha}\right) \frac{1}{\epsilon}\right). \end{aligned}$$

□

5 Numerical Experiments

We compare through numerical experiments the proposed adaptive algorithm to two other algorithms, the maximum likelihood amplitude estimation (MLAE) and the iterative quantum amplitude estimation (IQAE). We use the MLAE and IQAE algorithms provided in Qiskit, an open source software development kit for quantum computing. For comparison purposes, we also use quantum simulators and circuits in Qiskit when implementing the adaptive algorithm. In all algorithms X_t is sampled from a binomial distribution with probability $\sin^2((2m_t + 1)\theta)$ (with proper adjustment on θ in the adaptive algorithm). Therefore, the time costs reported below reflect the computation complexity of the classical part of the algorithms. We choose the confidence level as 95% in all algorithms. For IQAE and the adaptive algorithm, we set the target precision as $\{10^{-3}, 10^{-4}, \dots, 10^{-10}\}$. Instead of specifying the target precision, MLAE requires an input of the number of iterations T and chooses $\{m_t\}_{t=0}^T$ as $m_0 = 0, m_1 = 2^0, \dots, m_T = 2^{T-1}$. We use $T = 8, 10, 12$ and 14 . Furthermore, we choose $K = 3$ in the adaptive algorithm.

We compare the algorithms in three scenarios. We choose $N_{\text{shots}} = 100$ in all algorithms in the first two scenarios. In the first scenario, we sample 100 values of p uniformly from 0 to 0.5. Each point in Panel (a) (b) and (c) of Figure 2 is an average from the 100 experiments. The findings are summarized as follows. Firstly, from Panel (a) the adaptive algorithm requires slightly more oracle queries than MLAE and IQAE to achieve the same level of precision. MLAE uses the likelihood-ratio method to construct the confidence interval, which lacks for rigorous justification. When implementing IQAE, we chose the Clopper-Pearson method, which was not justified completely analytically (Supplementary information to Grinko et al. (2021), Theorem 1). We attempted to conduct experiments using IQAE with the Chernoff-Hoeffding method, which gives more conservative but theoretically justifiable intervals and is in line with the choice in the adaptive method. But the Qiskit version of IQAE with the Chernoff-Hoeffding method using $N_{\text{shots}} = 100$ could

not produce outcomes within a reasonable time. We will increase N_{shots} in the third scenario for comparison.

Secondly, the time costs of the classical part of the adaptive algorithm are substantially less than MLAE and IQAE from Panel (b). By Suzuki et al. (2020), the computational complexity⁶ of the classical part of MLAE is $O(1/\epsilon \log(1/\epsilon))$, which is in line with Panel (b). Due to its high time costs, we will not compare MLAE in the following scenarios. By contrast, the computational complexity of the classical part of the adaptive algorithm is $O(\log(1/\epsilon) \log(\log(1/\epsilon)))$ because T is $O(\log(1/\epsilon))$ and the runtime in each step t is proportional to the iterations in the **repeat** loop, which is $O(\log(\log(1/\epsilon)))$ by Theorem 1. The time costs of IQAE show a similar pattern but the average time cost is approximately 40 times of the adaptive algorithm.

Thirdly, we report the average value of r_t and the worst-case value, i.e., the smallest value across all steps. We gave a theoretical lower bound of r_t as $1/4$ in (11). From Panel (c), the average value of r_t is close to 1 and increases with the precision, which implies that the estimation loses very little efficiency due to the adjustment on average. The worst-case value is between 0.6 and 0.7.

Finally (not shown in the figure), 100% of the intervals by the adaptive algorithm and IQAE contain the true values of p in all experiments, and 98.5% of the intervals by MLAE contain the true values of p .

In the second scenario, we compare the adaptive algorithm and IQAE at a specific value $p = 0.25$, which corresponds to $\theta = \pi/6$, a boundary between periods of $\sin^2(K^t\theta)$ for $K = 3$. Each point in Panel (d) (e) and (f) of Figure 2 is an average from the 100 experiments. As before, 100% of the intervals by the adaptive algorithm and IQAE contain the true values of p in all experiments. The gaps between the numbers of oracle queries of the two methods becomes slightly larger. But a more notable pattern is the rapid growth of the runtime of IQAE when ϵ is small. The bottleneck of IQAE is the sub-routine FINDNEXTK, which performs the following task (using the notation in this paper): recall that m_{t+1} is the largest integer such that $|\theta_t^L - \theta_t^U| \leq \frac{1}{2m_{t+1}+1} \frac{\pi}{2}$. The sub-routine starts from m_{t+1} and gradually decreases this number until reach \tilde{m}_{t+1} such that $[\theta_t^L, \theta_t^U]$ is fully contained in a single length- $\frac{1}{2\tilde{m}_{t+1}+1} \frac{\pi}{2}$ period of $\sin^2((2\tilde{m}_{t+1} + 1)\theta)$. In the worst-case scenario, the runtime of FINDNEXTK can be proportional to m_{t+1} and eventually be $O(1/\epsilon)$, which is demonstrated in Panel (e). Finally, the adjustment factor r_t , especially in the worst-case scenario, is smaller than the corresponding value in the previous simulation. That is because $[\theta_t^L, \theta_t^U]$ is more likely to overlap with two periods since θ is at the boundary.

In the third scenario, we compare the adaptive algorithm and IQAE with the Clopper-Pearson method (IQAE_{CP}) and the Chernoff-Hoeffding method (IQAE_{CH}). We use $N_{\text{shots}} = 800$ in all three methods for a fair comparison because IQAE with the Chernoff-Hoeffding method using a smaller N_{shots} sometimes could not return an output. The rest of the setup is identical to the first scenario. As aforementioned, the Chernoff-Hoeffding method gives a more conservative confidence interval but with a theoretical guarantee. The same method is also used in the adaptive algorithm. From Figure 3, the number of oracle queries by the adaptive algorithm is between IQAE_{CP} and IQAE_{CH} under the same level of precision. This suggests that the adaptive algorithm uses a slightly smaller number of queries than IQAE when using the same method for constructing confidence intervals of $\sin^2((2m_t + 1)\theta)$. Moreover, the classical part of the adaptive algorithm has substantially lower

⁶Here we treat α as a constant.

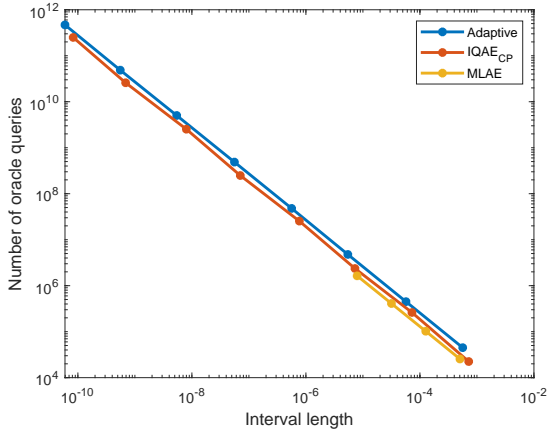
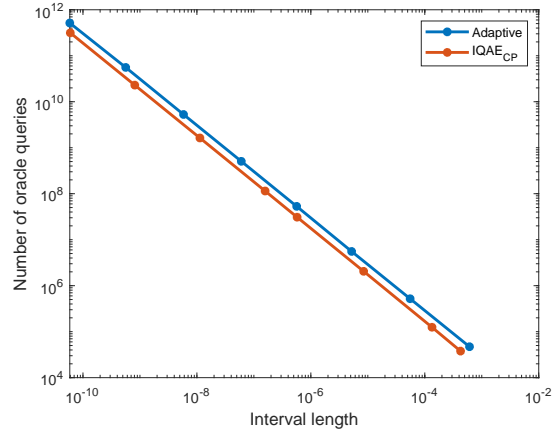
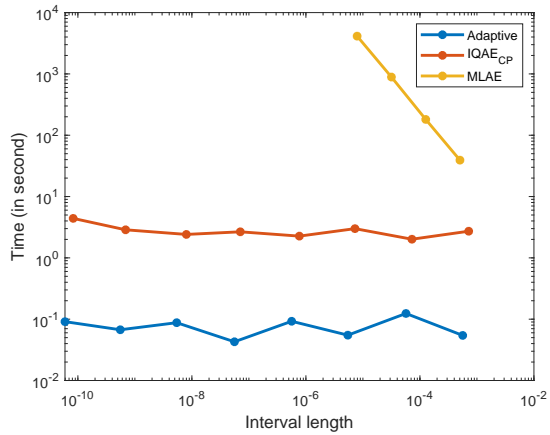
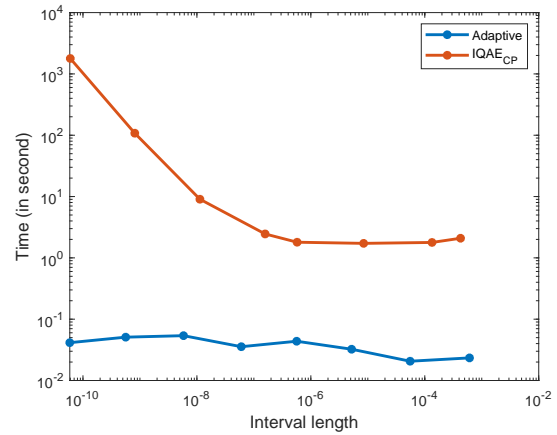
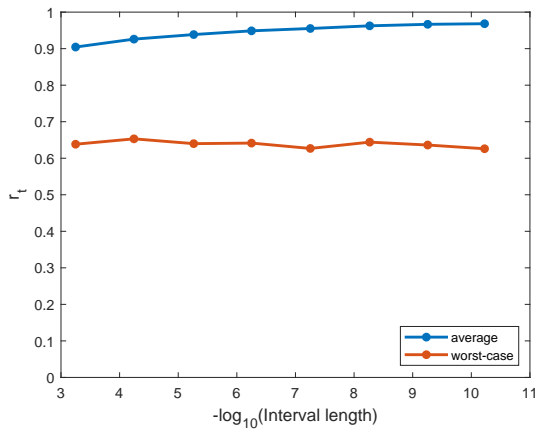
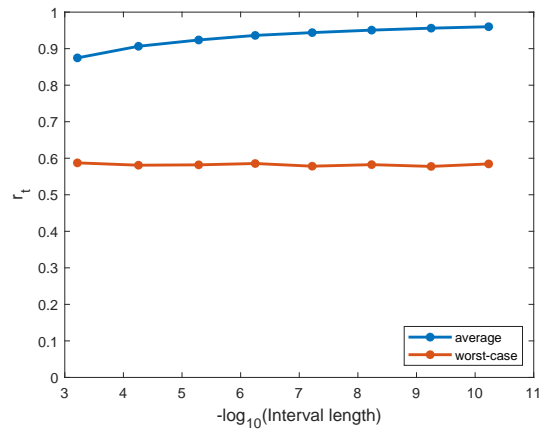
(a) Log-log plot of N_{oracles} for $p \sim U(0, 0.5)$ (d) Log-log plot of N_{oracles} for $p = 0.25$ (b) Log-log plot of time costs for $p \sim U(0, 0.5)$ (e) Log-log plot of time costs for $p = 0.25$ (c) Adjustment factor r_t for $p \sim U(0, 0.5)$ (f) Adjustment factor r_t for $p = 0.25$ 

Figure 2: Comparison of MLAE, IQAE, and the adaptive algorithm using $N_{\text{shots}} = 100$. Confidence level = 95%. Each point in Panel (a) (b) and (c) is an average of the experimental results for 100 values of p sampled from $U(0, 0.5)$. Each point in Panel (d) (e) and (f) is an average of 100 experimental results for $p = 0.25$. The average r_t refers to the average value of r_t over $t = 0, \dots, T$ and the worst-case r_t refers to the minimum value of r_t over $t = 0, \dots, T$.

computational complexity than IQAE as in the previous scenarios. Finally, 100% of the intervals by the adaptive algorithm and both versions of IQAE contain the true values of p in all experiments.

(a) Log-log plot of N_{oracles} for $p \sim U(0, 0.5)$ (d) Log-log plot of time costs for $p \sim U(0, 0.5)$

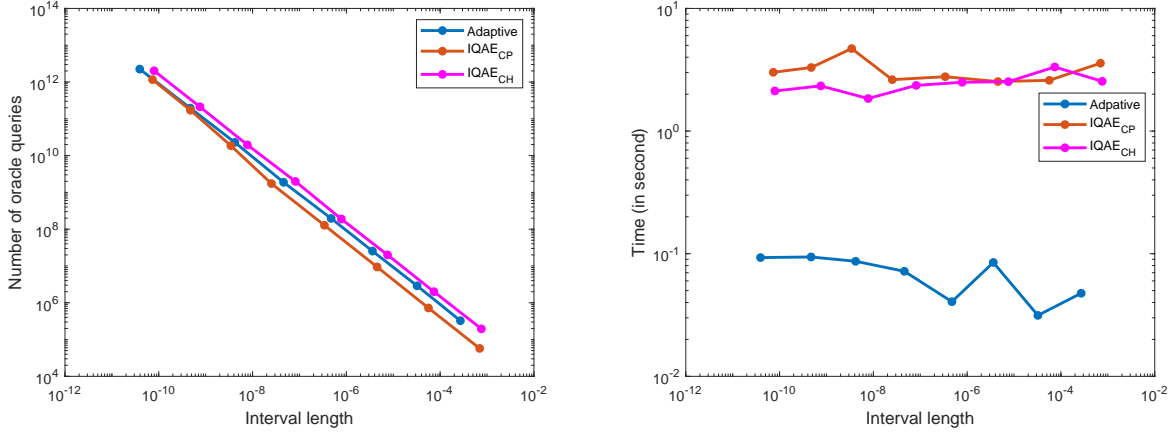


Figure 3: Comparison of MLAE, IQAE with the Clopper-Pearson method (IQAE_{CP}), and IQAE with the Chernoff-Hoeffding method (IQAE_{CH}) using $N_{\text{shots}} = 800$. Confidence level = 95%. Each point is an average of the experimental results for 100 values of p sampled from $U(0, 0.5)$.

6 Conclusion

We proposed a new Grover-based amplitude estimation algorithm. The number of oracle queries achieves $O(1/\epsilon)$ and the computational complexity of the classical part achieves $O(\log(1/\epsilon))$, both up to a double-logarithmic factor. The key ingredient of the algorithm is an adjustment factor r_t such that the confidence interval for $\theta_t = \arcsin \sqrt{r_t p}$ is fully contained in a single period as long as the length of the original interval for θ does not exceed the length of the period. With this adjustment, the algorithm does not need to search for the appropriate number of Grover iterations in each step, which can be time-consuming, and both the number of total steps and the number of measurements are easy to bound analytically.

The theoretical result in this paper (Theorem 1) is a non-asymptotic result in nature. In fact, such a non-asymptotic result is easier to formulate than an asymptotic result in this scenario because the number of measurements in a single step does not go to infinity. Therefore, a non-asymptotic bound such as Hoeffding's inequality can be naturally applied. But such a non-asymptotic bound can be loose. One may therefore be interested in the asymptotic distribution of $N_{\text{oracles}}(\hat{p} - p)$ where \hat{p} is an estimator of p such as the maximum likelihood estimator. A related but simpler problem is to derive the asymptotic variance of the estimator.

Appendix

Lemma 1. For $0 \leq \theta_1, \theta_2 \leq \pi/2$, $0 \leq r \leq 1$,

$$|\arcsin \sqrt{r(\sin \theta_1)^2} - \arcsin \sqrt{r(\sin \theta_2)^2}| \leq |\theta_1 - \theta_2|.$$

Proof. Without loss of generality, assume $\theta_1 > \theta_2$. Let

$$g(r) = \arcsin \sqrt{r(\sin \theta_1)^2} - \arcsin \sqrt{r(\sin \theta_2)^2}.$$

Note that $g(1) = \theta_1 - \theta_2$. Then we only need to prove $g(r)$ is a non-decreasing function. In fact,

$$\begin{aligned} g'(r) &= \frac{1}{\sqrt{1-r(\sin \theta_1)^2}} \sin \theta_1 \frac{1}{2\sqrt{r}} - \frac{1}{\sqrt{1-r(\sin \theta_2)^2}} \sin \theta_2 \frac{1}{2\sqrt{r}} \geq 0 \\ \Leftrightarrow \frac{\sin \theta_1}{\sqrt{1-r(\sin \theta_1)^2}} &\geq \frac{\sin \theta_2}{\sqrt{1-r(\sin \theta_2)^2}} \\ \Leftrightarrow (\sin \theta_1)^2(1-r(\sin \theta_2)^2) &\geq (\sin \theta_2)^2(1-r(\sin \theta_1)^2) \\ \Leftrightarrow (\sin \theta_1)^2 &\geq (\sin \theta_2)^2. \end{aligned}$$

□

Lemma 2. For $0 \leq \theta_1, \theta_2 \leq \pi/2$, $s \geq 1$, satisfying $s(\sin \theta_1)^2 \leq 1/2$ and $s(\sin \theta_2)^2 \leq 1/2$,

$$|\arcsin \sqrt{s(\sin \theta_1)^2} - \arcsin \sqrt{s(\sin \theta_2)^2}| \leq \sqrt{2s}|\theta_1 - \theta_2|.$$

Proof.

$$\left| \arcsin \sqrt{s(\sin \theta_1)^2} - \arcsin \sqrt{s(\sin \theta_2)^2} \right| = \left| \frac{\sqrt{s} \cos(\tilde{\theta})}{\sqrt{1-s(\sin \tilde{\theta})^2}} (\theta_1 - \theta_2) \right| \leq \sqrt{2s}|\theta_1 - \theta_2|.$$

□

Lemma 3. For $0 \leq p_1, p_2 \leq 1$,

$$|\arcsin \sqrt{p_1} - \arcsin \sqrt{p_2}| \leq \arcsin \sqrt{|p_1 - p_2|}.$$

Proof. Let $x = p_2$ and $\delta = p_1 - p_2$. Without loss of generality, assume $0 < \delta < 1$. Consider the function $f(x) = \arcsin \sqrt{x + \delta} - \arcsin \sqrt{x}$. We only need to prove

$$\max_{x \in [0, 1-\delta]} f(x) = f(0).$$

Notice

$$f'(x) = \frac{1}{2\sqrt{x+\delta}\sqrt{1-(x+\delta)}} - \frac{1}{2\sqrt{x}\sqrt{1-x}}.$$

The only stationary point of $f(x)$ on $[0, 1-\delta]$ is $x = \frac{1}{2}(1-\delta)$. Moreover, $\lim_{x \rightarrow 0} f'(x) = -\infty$ and $\lim_{x \rightarrow 1-\delta} f'(x) = \infty$. By the intermediate value theorem, $f'(x) < 0$ for $x \in (0, \frac{1}{2}(1-\delta))$ and $f'(x) > 0$ for $x \in (\frac{1}{2}(1-\delta), 1-\delta)$. By the mean value theorem, for all $x \in (0, \frac{1}{2}(1-\delta)]$, $f(x) - f(0) = xf'(\tilde{x}) < 0$ where $\tilde{x} \in (0, x)$. Similarly, for $x \in [\frac{1}{2}(1-\delta), 1-\delta)$, $f(1-\delta) - f(x) > 0$. Therefore, the maximum value of $f(x)$ can only be achieved at the two endpoints. In fact, $f(0) = f(1-\delta) = \arcsin \sqrt{\delta}$. □

References

- Aaronson, S. and Rall, P. (2020). Quantum approximate counting, simplified. In *Symposium on Simplicity in Algorithms*, pages 24–32. SIAM.
- Ambainis, A. (2004). Quantum search algorithms. *ACM SIGACT News*, 35(2):22–35.
- Artiles, L. M., Gill, R. D., and Guță, M. I. (2005). An invitation to quantum tomography. *Journal of the Royal Statistical Society. Series B (Statistical Methodology)*, 67(1):109–134.
- Brassard, G., Hoyer, P., Mosca, M., and Tapp, A. (2002). Quantum amplitude amplification and estimation. *Contemporary Mathematics*, 305:53–74.
- Cao, Y., Romero, J., Olson, J. P., Degroote, M., Johnson, P. D., Kieferová, M., Kivlichan, I. D., Menke, T., Peropadre, B., Sawaya, N. P., et al. (2019). Quantum chemistry in the age of quantum computing. *Chemical reviews*, 119(19):10856–10915.
- Durr, C. and Hoyer, P. (1996). A quantum algorithm for finding the minimum. *arXiv preprint quant-ph/9607014*.
- Egger, D. J., Gutiérrez, R. G., Mestre, J. C., and Woerner, S. (2020). Credit risk analysis using quantum computers. *IEEE Transactions on Computers*, 70(12):2136–2145.
- Gill, R. D. (2008). Conciliation of bayes and pointwise quantum state estimation. In *Quantum Stochastics and Information: Statistics, Filtering and Control*, pages 239–261. World Scientific.
- Gill, R. D. and Guță, M. I. (2013). On asymptotic quantum statistical inference. In *From Probability to Statistics and Back: High-Dimensional Models and Processes—A Festschrift in Honor of Jon A. Wellner*, pages 105–127. Institute of Mathematical Statistics.
- Grinko, D., Gacon, J., Zoufal, C., and Woerner, S. (2021). Iterative quantum amplitude estimation. *npj Quantum Information*, 7(1):1–6.
- Grover, L. K. (1996). A fast quantum mechanical algorithm for database search. In *Proceedings of the twenty-eighth annual ACM symposium on Theory of computing*, pages 212–219.
- Herman, D., Googin, C., Liu, X., Galda, A., Safro, I., Sun, Y., Pistoia, M., and Alexeev, Y. (2022). A survey of quantum computing for finance. *arXiv preprint arXiv:2201.02773*.
- Hoeffding, W. (1963). Probability inequalities for sums of bounded random variables. *Journal of the American Statistical Association*, 58(301):13–30.
- Hong, L. J., Hu, Z., and Liu, G. (2014). Monte carlo methods for value-at-risk and conditional value-at-risk: a review. *ACM Transactions on Modeling and Computer Simulation (TOMACS)*, 24(4):1–37.
- Hu, J. and Wang, Y. (2020). Quantum annealing via path-integral monte carlo with data augmentation. *Journal of Computational and Graphical Statistics*, 30(2):284–296.
- Kassal, I., Jordan, S. P., Love, P. J., Mohseni, M., and Aspuru-Guzik, A. (2008). Polynomial-time quantum algorithm for the simulation of chemical dynamics. *Proceedings of the National Academy of Sciences*, 105(48):18681–18686.

- Kitaev, A. Y. (1995). Quantum measurements and the abelian stabilizer problem. *arXiv preprint quant-ph/9511026*.
- Knill, E., Ortiz, G., and Somma, R. D. (2007). Optimal quantum measurements of expectation values of observables. *Physical Review A*, 75(1):012328.
- Kochenberger, G., Hao, J.-K., Glover, F., Lewis, M., Lü, Z., Wang, H., and Wang, Y. (2014). The unconstrained binary quadratic programming problem: a survey. *Journal of combinatorial optimization*, 28(1):58–81.
- Montanaro, A. (2015). Quantum speedup of monte carlo methods. *Proceedings of the Royal Society A: Mathematical, Physical and Engineering Sciences*, 471(2181):20150301.
- Nakaji, K. (2020). Faster amplitude estimation. *arXiv preprint arXiv:2003.02417*.
- Nielsen, M. A. and Chuang, I. (2011). *Quantum Computation and Quantum Information: 10th Anniversary Edition*. Cambridge University Press.
- Pomerance, C. (1996). A tale of two sieves. In *Notices Amer. Math. Soc.* Citeseer.
- Ramezani, S. B., Sommers, A., Manchukonda, H. K., Rahimi, S., and Amirlatifi, A. (2020). Machine learning algorithms in quantum computing: A survey. In *2020 international joint conference on neural networks (IJCNN)*, pages 1–8. IEEE.
- Rebentrost, P., Gupt, B., and Bromley, T. R. (2018). Quantum computational finance: Monte carlo pricing of financial derivatives. *Physical Review A*, 98(2):022321.
- Shor, P. W. (1994). Algorithms for quantum computation: discrete logarithms and factoring. In *Proceedings 35th annual symposium on foundations of computer science*, pages 124–134. Ieee.
- Sun, G., Su, S., and Xu, M. (2014). Quantum algorithm for polynomial root finding problem. In *2014 Tenth International Conference on Computational Intelligence and Security*, pages 469–473. IEEE.
- Suzuki, Y., Uno, S., Raymond, R., Tanaka, T., Onodera, T., and Yamamoto, N. (2020). Amplitude estimation without phase estimation. *Quantum Information Processing*, 19(2):1–17.
- Wang, Y. (2022). When quantum computation meets data science: Making data science quantum. *Harvard Data Science Review*, 4(1). <https://hdsr.mitpress.mit.edu/pub/kpn45eyx>.
- Wang, Y. and Liu, H. (2022). Quantum computing in a statistical context. *Annual Review of Statistics and Its Application*, 9.
- Wang, Y., Wu, S., and Zou, J. (2016). Quantum annealing with markov chain monte carlo simulations and d-wave quantum computers. *Statistical Science*, pages 362–398.
- Wie, C.-R. (2019). Simpler quantum counting. *Quantum Information & Computation*, 16(11-12):967–983.
- Wiebe, N., Kapoor, A., and Svore, K. M. (2015). Quantum algorithms for nearest-neighbor methods for supervised and unsupervised learning. *Quantum Information & Computation*, 15(3-4):316–356.

- Wiebe, N., Kapoor, A., and Svore, K. M. (2016). Quantum deep learning. *Quantum Information & Computation*, 16(7-8):541–587.
- Woerner, S. and Egger, D. J. (2019). Quantum risk analysis. *npj Quantum Information*, 5(1):1–8.
- Zhong, W., Ke, Y., Wang, Y., Chen, Y., Chen, J., and Ma, P. (2021). Best subset selection: Statistical computing meets quantum computing. *arXiv preprint arXiv:2107.08359*.
- Zoufal, C., Lucchi, A., and Woerner, S. (2019). Quantum generative adversarial networks for learning and loading random distributions. *npj Quantum Information*, 5(1):1–9.